Acta Materialia 115 (2016) 314–323

Contents lists available at ScienceDirect

Acta Materialia

journal homepage: www.elsevier.com/locate/actamat

Full length article

Quantification of dislocation structures from anelastic deformation behaviour

Zaloa Arechabaleta [a, *], Peter van Liempt [b], Jilt Sietsma [a]

[a] Department of Materials Science and Engineering, Delft University of Technology, Mekelweg 2, 2628 CD, Delft, The Netherlands
[b] Tata Steel Research, Development and Technology, Postbus 10000 (3G37), 1970 CA, IJmuiden, The Netherlands

A R T I C L E I N F O

Article history:
Received 18 March 2016
Received in revised form
24 May 2016
Accepted 25 May 2016

Keywords:
Anelastic strain
Dislocation structure
Tensile test
X-ray diffraction

A B S T R A C T

The pre-yield deformation behaviour (i.e., at stresses below the yield stress) of two materials, pure iron and a low-alloy steel, and its anelastic nature are analysed at room temperature, before and after the dislocation structures are varied by plastic deformation. It is shown, based on tensile experiments, that this behaviour can be explained by limited reversible glide of dislocations without essential changes in the dislocation structure. Moreover, a physically-based model that characterises the dislocation structure by two variables, the dislocation density and the effective dislocation segment length, is used to quantitatively describe this deformation behaviour. The model validity is further evaluated by comparison with dislocation densities from X-Ray Diffraction measurements.

1. Introduction

Sheet metal forming processes are extensively used in many sectors. Yet, the dimensional control of the formed sheets is a real challenge: springback -defined as the strain relaxation after release of the forming stresses- cannot be predicted accurately. Experimental evidence has shown that the magnitude of springback is not only dependent on the elastically recovered strain, but also on an anelastic contribution to the total relaxed strain [1–3]. The former, determined by the atomic interactions, is given by Hooke's law, whereas the latter is caused by dislocations within the material [1,4]. However, how do the dislocations cause this anelasticity? Already below the yield stress, dislocation segments bow out, causing an additional strain component, and thus the well-known reduction of the Young's modulus after plastic deformation [2,5,6]. This additional strain component is defined in this study as anelastic strain, according to [4,7], and is responsible for the non-linearity that is often observed in the stress-strain curve regime below the yield stress. If the load is released at any stage before the material starts to yield, this behaviour is reversible and the dislocations return to an equilibrium configuration. Once the yield stress is reached, Frank-Read sources are activated and the dislocations multiply. After plastic deformation and during unloading, the mobile dislocations move in the reverse direction, so similar mechanisms as those occurring in the pre-yield regime (with an increased dislocation density) are expected to reverse the anelastic strain, and lead to the springback phenomenon. Anelastic strain, as it is defined here, is related to the dislocations' subcritical bowing during loading and reversible bowing during unloading [8,9], which are essentially time independent at room temperature.

A better comprehension of the anelastic dislocation behaviour is essential for a complete physical model of the pre-yield behaviour of metals. Recently, a dislocation based model has been developed by van Liempt et al. [1] to account for the anelastic deformation in the pre-yield regime. The model, summarised in Section 2, quantifies the anelastic contribution as a function of two variables that characterise the dislocation structure in the material: the dislocation density and the effective dislocation segment length.

In this work, the pre-yield deformation behaviour of two materials, pure iron and a low-alloy steel, is analysed at room temperature using tensile tests. It is seen that this behaviour can be adequately explained by considering that, besides elastic strain, limited glide of dislocations does occur below the yield stress. The experimental results are discussed and quantified in relation with the predictions by the model for anelastic deformation. The model is validated by means of X-Ray Diffraction (XRD), by comparison of the dislocation density values obtained through the model

* Corresponding author.
E-mail addresses: z.arechabaletaguenechea@tudelft.nl (Z. Arechabaleta), peter.van-liempt@tatasteel.com (P. van Liempt), j.sietsma@tudelft.nl (J. Sietsma).

http://dx.doi.org/10.1016/j.actamat.2016.05.040
1359-6454/

application to the tensile curves with the values from the XRD analysis.

2. Anelastic behaviour of dislocations

During loading in the pre-yield regime, purely elastic strain due to atomic interactions, ε_e, and anelastic strain due to bowing-out of dislocation segments, ε_a, are simultaneously occurring, so the total strain ε_{pre} can be described as the sum of both contributions:

$$\varepsilon_{pre} = \varepsilon_e + \varepsilon_a = (\sigma/E) + \varepsilon_a \tag{1}$$

where σ is the applied stress and E is the elastic modulus of the crystal lattice. The stiffness in the pre-yield regime can be characterised by the derivative of the previous equation, which is:

$$\Theta_{pre} = \mathrm{d}\sigma/\mathrm{d}\varepsilon_{pre} = E\Theta_a/(E+\Theta_a) \tag{2}$$

where Θ_{pre} is the slope of the pre-yield stress-strain curve and $\Theta_a = \mathrm{d}\sigma/\mathrm{d}\varepsilon_a$ is the anelastic contribution to the pre-yield deformation behaviour. The latter is determined by the dislocation structure and behaviour. In order to analyse this behaviour, we consider a dislocation segment of length l pinned by other dislocation nodes, solute atoms or precipitates, as in Fig. 1(a). An applied shear stress τ causes the dislocation segment, initially at rest, to bow out and produce slip under the action of a glide force (Fig. 1(b)). This (limited) dislocation motion causes the anelastic strain. For N dislocation segments of length l per unit volume, the total anelastic shear strain γ_a can be expressed as:

$$\gamma_a = NbA \tag{3}$$

in which b is the length of the Burgers vector and A is the area swept by each dislocation. This area can be determined using the expression for a circle segment area:

$$A = \frac{1}{2}r^2(\varphi - \sin\varphi) \tag{4}$$

in which r is the radius of curvature and φ is the subtended angle (see Fig. 1(b)). In order to determine the anelastic contribution for any stress value within $0 < \sigma \leq \sigma_y$, the exact expression for the subtended angle φ is used:

$$\varphi = 2\arcsin(l/2r) \tag{5}$$

The only force that opposes the applied shear stress τ is the back stress due to the line tension of the dislocation, $T = Gb/2r$, where G is the shear modulus. For a small applied stress, the dislocation segment reaches an equilibrium position when $\tau = T$. The radius of curvature is then given by:

$$r = Gb/2\tau \tag{6}$$

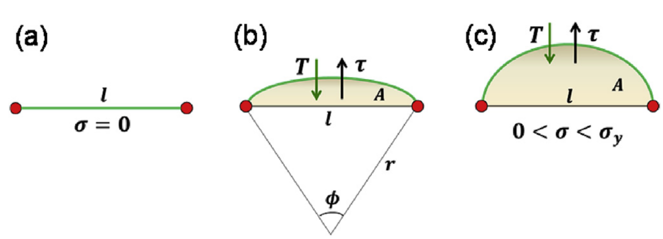

Fig. 1. Scheme of the bow-out mechanism of a dislocation below the yield stress. (a) The dislocation at an equilibrium configuration, (b) and (c) after bowing out to different curvatures.

As the shear stress τ increases, the area A swept by the dislocation and thus the anelastic strain γ_a increase. This process, as pointed out before, is reversible below the yield stress. At the yield stress, however, the radius of curvature r reaches its minimum ($r_{min} = l/2$) and the bowing-out becomes instable. Beyond this point, Equation (6) is no longer satisfied and dislocation loops start to form from the Frank-Read source. Plastic deformation has then begun. Consequently, the yield stress σ_y can be defined as the critical stress σ_c above which the bow-out mechanism is non-reversible. The yield stress σ_y can therefore be expressed by:

$$\sigma_y = \sigma_c = \overline{M}Gb/l \tag{7}$$

where $\overline{M}$ is the Taylor factor. Using Equations (3)–(7), the anelastic contribution can be determined in the entire pre-yield regime as follows [1]:

$$\Theta_a = \mathrm{d}\sigma/\mathrm{d}\varepsilon_a = \left[\overline{M}^2Es^3\sqrt{(1-s^2)}\right] \Big/ \left[\rho l^2(1+\nu)\left(s - \sqrt{(1-s^2)}\arcsin s\right)\right] \tag{8}$$

where s is the stress normalised by the critical stress, $s = \sigma/\sigma_c$, ρ is the dislocation density and ν is Poisson's ratio. It must be noticed here that $Nl^3 = \rho l^2$. Finally, the pre-yield stiffness is obtained, substituting Equation (8) into Equation (2), as:

$$\Theta_{pre} = \frac{\overline{M}^2Es^3\sqrt{(1-s^2)}}{\overline{M}^2s^3\sqrt{(1-s^2)} + \rho l^2(1+\nu)\left(s-\sqrt{(1-s^2)}\arcsin s\right)} \tag{9}$$

It should be noted that the lengths of dislocation segments in a real material will form a distribution, which will cause the yield stress not to be a single value. The parameter l in the model description should be regarded as an effective value related to the effective average yield stress. Longer segments will be activated as Frank-Read sources at somewhat lower stress, shorter segments at higher stress. The extension of the yield-stress range is directly related to the width of the segment-length distribution. A wider segment-length distribution will cause a more gradual transition between the pre-yield and post-yield ranges in the extended Kocks-Mecking plot (see Section 4.1).

3. Experimental procedure

3.1. Materials

Two materials, with chemical compositions listed in Table 1, were selected for this study: pure iron (ARMCO pure iron, cold rolled and subsequently annealed, provided by AK Steel International) and a low-alloy steel (99.5% iron foil, as-rolled, provided by Goodfellow Cambridge Ltd.). The microstructure of the as-received materials was characterised by optical microscopy and the grain size was measured according to the equivalent diameter procedure. Fig. 2 shows the ferritic microstructures, which were revealed using a 2%Nital solution, together with the grain size measured in each case. The rolling and transverse directions (designated as RD and TD, respectively) are indicated. From the micrographs, it can be noticed that the pure iron exhibits a larger grain size than the steel, that is, 27 vs. 11 μm. Additional analysis revealed that there is no significant texture, and consequently, grains can be considered randomly oriented for both materials.